DEVELOPMENT OF TWO NEW AUXILIARY INFORMATION CONTROL CHARTS, AND ECONOMIC AND ECONOMIC-STATISTICAL DESIGNS OF SEVERAL AUXILIARY INFORMATION CONTROL CHARTS

NG PEH SANG

UNIVERSITI SAINS MALAYSIA

2020

DEVELOPMENT OF TWO NEW AUXILIARY INFORMATION CONTROL CHARTS, AND ECONOMIC AND ECONOMIC-STATISTICAL DESIGNS OF SEVERAL AUXILIARY INFORMATION CONTROL CHARTS

by

NG PEH SANG

Thesis submitted in fulfillment of the requirements for the degree of Doctor of Philosophy

July 2020

ACKNOWLEDGEMENT

First and foremost, I would like to take this opportunity to express my deepest and sincere gratitude to my supervisor, Prof. Michael Khoo Boon Chong, for his constant guidance, insightful suggestions, ideas and continuous encouragements throughout my study. His invaluable knowledge, profound experience and expertise in Statistical Quality Control (SQC) has enabled me to complete my Ph.D. research successfully. I am deeply indebted to him for his willingness to spend his precious time in guiding me, responding to my queries promptly and checking my research work thoroughly.

I have great pleasure in acknowledging my gratitude to the Ministry of Higher Education for awarding me with the MyPhD scholarship, which has provided financial support throughout my Ph.D. study. My sincere thanks also goes to Prof. Hailiza Kamarulhaili, Dean of the School of Mathematical Sciences, USM, for her assistance and support in my postgraduate study. Also, special thanks go to the lecturers and staff of the School of Mathematical Sciences, librarians, as well as those who have contributed to the completion of this study.

My acknowledgements would be incomplete without thanking the biggest source of my strength, i.e. my parents and sister, for their spiritual support, endless love and continuous encouragement throughout my life. I thank them for always supporting me in difficult moments. Also, I would like to thank all my friends who have rendered me their assistance, friendship and moral support. I am indebted to all of you from the bottom of my heart. Last but not least, I would like to offer my sincere thanksgiving to Buddha for all of his blessings.

Peh Sang
July 2020

TABLE OF CONTENTS

LIST OF TABLES

LIST OF FIGURES

LIST OF ABBREVIATIONS

ARL	Average run length
ARL_0	In-control ARL
$\text{ARL}(\delta)$	Out-of-control ARL
ATS	Average time to signal
ATS_0	In-control ATS
$\text{ATS}(\delta)$	Out-of-control ATS
cdf	Cumulative distribution function
CL	Center line
$\text{CL}_{(\text{RS } \bar{X})}$	CL of RS $\bar{X}$ chart
$\text{CL}_{(\text{RS } \bar{X} \text{ - AI})}$	CL of RS $\bar{X}$ - AI chart
$\text{CL}_{(\text{VSI EWMA } t)}$	CL of VSI EWMA *t* chart
$\text{CL}_{(\text{VSI EWMA } t \text{ - AI})}$	CL of VSI EWMA *t* - AI chart
CRL	Conforming run length
CUSUM	Cumulative sum
EARL	Expected ARL
EARL_0	In-control EARL
$\text{EARL}(\delta_{\min}, \delta_{\max})$	Out-of-control EARL
EATS	Expected ATS
EATS_0	In-control EATS
$\text{EATS}(\delta_{\min}, \delta_{\max})$	Out-of-control EATS

EWMA	Exponentially weighted moving average
EWMA $\bar{X}$ - AI	EWMA $\bar{X}$ auxiliary information
EWMA t - AI	EWMA t auxiliary information
LCL	Lower control limit
$\text{LCL}_{(\bar{X}\text{ - AI})}$	LCL of $\bar{X}$ - AI chart
$\text{LCL}_{(\text{EWMA } \bar{X}\text{ - AI})}$	LCL of EWMA $\bar{X}$ - AI chart
$\text{LCL}_{(\text{EWMA } t\text{ - AI})}$	LCL of EWMA t - AI chart
$\text{LCL}_{(\text{VSI EWMA } t)}$	LCL of VSI EWMA t chart
$\text{LCL}_{(\text{VSI EWMA } t\text{ - AI})}$	LCL of VSI EWMA t - AI chart
$\text{LCL}_{(\text{RS } \bar{X})}$	LCL of RS $\bar{X}$ chart
$\text{LCL}_{(\text{RS } \bar{X}\text{ - AI})}$	LCL of RS $\bar{X}$ - AI chart
LWL	Lower warning limit
$\text{LWL}_{(\text{VSI EWMA } t)}$	LWL of VSI EWMA t chart
$\text{LWL}_{(\text{VSI EWMA } t\text{ - AI})}$	LWL of VSI EWMA t - AI chart
pdf	Probability density function
RATS	Relative ATS
REATS	Relative EATS
RS	Run sum
RS $\bar{X}$ - AI	RS $\bar{X}$ auxiliary information
SAS	Statistical Analysis Software
SDTS	Standard deviation of the time to signal
SDTS_0	In-control SDTS

$\mathrm{SDTS}(\delta)$	Out-of-control SDTS
SPC	Statistical Process Control
SYN $\bar{X}$ - AI	Synthetic $\bar{X}$ auxiliary information
tpm	Transition probability matrix
UCL	Upper control limit
$\mathrm{UCL}_{(\bar{X}\text{ - AI})}$	UCL of $\bar{X}$ - AI chart
$\mathrm{UCL}_{(\text{EWMA } \bar{X}\text{ - AI})}$	UCL of EWMA $\bar{X}$ - AI chart
$\mathrm{UCL}_{(\text{EWMA } t\text{ - AI})}$	UCL of EWMA t - AI chart
$\mathrm{UCL}_{(\text{VSI EWMA } t)}$	UCL of VSI EWMA t chart
$\mathrm{UCL}_{(\text{VSI EWMA } t\text{ - AI})}$	UCL of VSI EWMA t - AI chart
$\mathrm{UCL}_{(\text{RS } \bar{X})}$	UCL of RS $\bar{X}$ chart
$\mathrm{UCL}_{(\text{RS } \bar{X}\text{ - AI})}$	UCL of RS $\bar{X}$ - AI chart
UWL	Upper warning limit
$\mathrm{UWL}_{(\text{VSI EWMA } t)}$	UWL of VSI EWMA t chart
$\mathrm{UWL}_{(\text{VSI EWMA } t\text{ - AI})}$	UWL of VSI EWMA t - AI chart
VSI	Variable sampling interval
VSI EWMA t - AI	VSI EWMA t auxiliary information
$\bar{X}$ - AI	Shewhart $\bar{X}$ auxiliary information

LIST OF NOTATIONS

$\Phi(\cdot)$	cdf of the standard normal distribution
n	Sample size
δ	Magnitude of the standardized mean shift
$\delta_{\max}$	Upper bound of the standardized mean shift
$\delta_{\min}$	Lower bound of the standardized mean shift
μ_0	In-control process mean
μ_{X0}	In-control process mean for the study variable X
μ_{X1}	Out-of-control process mean for the study variable X
μ_Y	Process mean for the auxiliary variable Y
σ_0	In-control process standard deviation
σ_X	Process standard deviation for the study variable X
σ_Y	Process standard deviation for the auxiliary variable Y
ρ	Correlation coefficient between the study variable X and auxiliary variable Y
$f_\delta(\delta)$	pdf of δ
$n_{(\bar{X}\text{ - AI})}$	Sample size of $\bar{X}$ - AI chart
$n_{(\text{SYN }\bar{X}\text{ - AI})}$	Sample size of SYN $\bar{X}$ - AI chart
$n_{(\text{EWMA }\bar{X}\text{ - AI})}$	Sample size of EWMA $\bar{X}$ - AI chart
$k_{(\bar{X}\text{ - AI})}$	Control limit coefficient of $\bar{X}$ - AI chart
$k_{(\text{SYN }\bar{X}\text{ - AI})}$	Control limit coefficient of SYN $\bar{X}$ - AI chart

$k_{(\text{EWMA } \bar{X} \text{ - AI})}$	Control limit coefficient of EWMA $\bar{X}$ - AI chart
$k_{(\text{EWMA } t \text{ - AI})}$	Control limit coefficient of EWMA t - AI chart
$k_{(\text{VSI EWMA } t)}$	Control limit coefficient of VSI EWMA t chart
$k_{(\text{VSI EWMA } t \text{ - AI})}$	Control limit coefficient of VSI EWMA t - AI chart
$h_{(\bar{X} \text{ - AI})}$	Sampling interval of $\bar{X}$ - AI chart
$h_{(\text{SYN } \bar{X} \text{ - AI})}$	Sampling interval of SYN $\bar{X}$ - AI chart
$h_{(\text{EWMA } \bar{X} \text{ - AI})}$	Sampling interval of EWMA $\bar{X}$ - AI chart
$L_{(\text{SYN } \bar{X} \text{ - AI})}$	Lower limit of CRL sub-chart of the SYN $\bar{X}$ - AI chart
$w_{(\text{VSI EWMA } t \text{ - AI})}$	Warning limit coefficient of VSI EWMA t - AI chart
$w_{(\text{VSI EWMA } t)}$	Warning limit coefficient of VSI EWMA t chart
$\lambda_{(\text{EWMA } \bar{X} \text{ - AI})}$	Smoothing constant of EWMA $\bar{X}$ - AI chart
$\lambda_{(\text{EWMA } t \text{ - AI})}$	Smoothing constant of EWMA t - AI chart
$\lambda_{(\text{VSI EWMA } t)}$	Smoothing constant of VSI EWMA t chart
$\lambda_{(\text{VSI EWMA } t \text{ - AI})}$	Smoothing constant of VSI EWMA t - AI chart
L	Lower limit of CRL sub-chart
$\boldsymbol{q}$	Steady state probability vector
$\boldsymbol{I}$	Identity matrix
$\mathbf{1}$	Vector where all elements are ones
$\boldsymbol{Q}_{(\text{EWMA } \bar{X} \text{ - AI})}$	tpm for the transient states of the Markov chain model of the EWMA $\bar{X}$ - AI chart
$\boldsymbol{Q}_{(\text{SYN } \bar{X} \text{ - AI})}$	tpm for the transient states of the Markov chain model of the SYN $\bar{X}$ - AI chart
$\boldsymbol{Q}_{(\text{RS } \bar{X})}$	tpm for the transient states of the Markov chain model of the RS $\bar{X}$ chart

$\boldsymbol{Q}_{(\text{VSI EWMA } t)}$	tpm for the transient states of the Markov chain model of the VSI EWMA *t* chart
$\boldsymbol{Q}_{(\text{RS } \bar{X} \text{ - AI})}$	tpm for the transient states of the Markov chain model of the RS $\bar{X}$ - AI chart
$\boldsymbol{Q}^{*}_{(\text{RS } \bar{X} \text{ - AI})}$	tpm with the absorbing state of the Markov chain model of the RS $\bar{X}$ - AI chart
$\boldsymbol{Q}^{*}_{(\text{SYN } \bar{X} \text{ - AI})}$	tpm with the absorbing state of the Markov chain model of the SYN $\bar{X}$ - AI chart
h	Sampling interval
h_1	Short sampling interval
h_2	Long sampling interval
$\boldsymbol{t}$	Vector of sampling intervals
b	Fixed cost per sample
c	Cost per unit sampled
C	Expected cost per unit of time
C_0	Expected cost per unit of time due to nonconformities produced while the process is in-control
C_1	Expected cost per unit of time due to nonconformities produced while the process is out-of-control
e	Expected time to sample and interpret one unit
s	Expected number of samples taken before an assignable cause occurs
T_0	Expected search time for a false alarm
T_1	Expected time to find the assignable cause
T_2	Expected time to repair the process
Y	Cost of a false alarm
W	Cost of removing an assignable cause

γ_1	= 1 if production continues during search
	= 0 if production stops during search
γ_2	= 1 if production continues during repair
	= 0 if production stops during repair
η	Process failure rate
τ	Expected time of occurrence of an assignable cause

PEMBANGUNAN DUA CARTA KAWALAN BERDASARKAN MAKLUMAT TAMBAHAN, DAN REKA BENTUK EKONOMI DAN EKONOMI-BERSTATISTIK UNTUK BEBERAPA CARTA KAWALAN BERDASARKAN MAKLUMAT TAMBAHAN

ABSTRAK

Penggunaan konsep baharu maklumat bantuan (AI) dalam carta kawalan menerima perhatian yang semakin meningkat di kalangan penyelidik. Carta kawalan dengan ciri maklumat tambahan telah ditunjukkan lebih berkesan daripada carta kawalan tanpa ciri tersebut. Ciri penting konsep AI telah mendorong kami untuk membangunkan dua carta AI baharu. Objektif pertama tesis ini adalah untuk membangunkan carta hasil tambah larian $\bar{X}$ - AI (RS $\bar{X}$ - AI) untuk pemantauan min proses. Parameter optimum yang dikira dengan menggunakan algoritma optimum yang dibangunkan dan pendekatan langkah demi langkah pembinaan carta RS $\bar{X}$ - AI optimum dipaparkan dalam tesis ini. Kriteria prestasi panjang larian purata (ARL) dan jangkaan panjang larian purata (EARL) digunakan untuk mengukur prestasi carta RS $\bar{X}$ - AI. Keputusan menunjukkan bahawa carta RS $\bar{X}$ - AI secara umumnya mempunyai prestasi yang lebih baik daripada carta $\bar{X}$ - AI, sintetik $\bar{X}$ - AI dan EWMA $\bar{X}$ - AI sedia ada dalam pengesanan isyarat luar kawalan. Objektif kedua tesis ini adalah untuk membangunkan carta selang pensampelan berubah purata bergerak berpemberat eksponen t AI (VSI EWMA t - AI) bagi pemantauan min proses apabila ralat dalam penganggaran sisihan piawai proses wujud. Carta VSI EWMA t - AI membenarkan sama ada selang pensampelan pendek atau panjang digunakan, berdasarkan maklumat kualiti proses daripada statistik semasa yang diplotkan pada

carta. Kriteria prestasi masa untuk berisyarat purata (ATS) dan jangkaan masa untuk berisyarat purata (EATS) digunakan untuk mengukur prestasi carta VSI EWMA t - AI, yang mana keputusan menunjukkan bahawa carta baharu ini adalah lebih baik daripada (i) carta EWMA t - AI sedia ada dalam pengesanan isyarat luar kawalan apabila sisihan piawai proses adalah terkawal dan (ii) carta EWMA $\bar{X}$ - AI sedia ada dengan menpunyai variasi yang lebih kecil bagi nilai-nilai ATS dan EATS (bagi saiz anjakan terpiawai ≤ 0.2) apabila sisihan piawai proses berubah. Pelaksanaan carta VSI EWMA t - AI ditunjukkan dengan menggunakan contoh berangka. Objektif ketiga tesis ini adalah untuk menyiasat prestasi ekonomi dan ekonomi-berstatistik carta $\bar{X}$ - AI, sintetik $\bar{X}$ - AI dan EWMA $\bar{X}$ - AI. Pengiraan parameter optimum carta-carta yang dinyatakan di atas dengan menggunakan algoritma pengoptimuman dan butiran terperinci reka bentuk ekonomi dan ekonomi-berstatistik carta-carta tersebut juga dibincangkan dalam tesis ini. Kriteria ARL and EARL digunakan untuk menetapkan prestasi berstatistik dalam kawalan dan luar kawalan carta-carta tersebut. Dengan menggabungkan reka bentuk ekonomi dan ekonomi-berstatistik dalam carta $\bar{X}$ - AI, sintetik $\bar{X}$ - AI dan EWMA $\bar{X}$ - AI, kos pelaksanaan carta-carta tersebut dapat diminimumkan.

DEVELOPMENT OF TWO NEW AUXILIARY INFORMATION CONTROL CHARTS, AND ECONOMIC AND ECONOMIC-STATISTICAL DESIGNS OF SEVERAL AUXILIARY INFORMATION CONTROL CHARTS

ABSTRACT

The use of auxiliary information (AI) concept in control charts is receiving increasing attention among researchers. Control charts with auxiliary characteristics have been shown to be more efficient than control charts without such characteristics. The salient feature of the AI concept has motivated us to develop two new AI charts. The first objective of this thesis is to develop the run sum $\bar{X}$ - AI (RS $\bar{X}$ - AI) chart for monitoring the process mean. Optimal parameters computed using the optimization algorithms developed and the step-by-step approach for constructing the optimal RS - AI chart are provided in this thesis. The average run length (ARL) and expected average run length (EARL) performance criteria are used to evaluate the performance of the RS $\bar{X}$ - AI chart. Results show that the RS $\bar{X}$ - AI chart generally surpasses the existing $\bar{X}$ - AI, synthetic $\bar{X}$ - AI and EWMA $\bar{X}$ - AI charts in the detection of out-of-control signals. The second objective of this thesis is to develop the variable sampling interval exponentially weighted moving average *t* AI (VSI EWMA *t* - AI) chart for monitoring the process mean when errors in estimating the process standard deviation exist. The VSI EWMA *t* - AI chart allows either the short or long sampling interval to be adopted, based on information from the process quality given by the current plotting statistic of the chart. The average time to signal (ATS) and expected average time to signal (EATS) performance criteria are used to evaluate the VSI

EWMA t - AI chart's performance, where results show that this new chart outperforms (i) the existing EWMA t - AI chart in the detection of out-of-control signals when the process standard deviation is in-control and (ii) the existing EWMA $\bar{X}$ - AI chart by having smaller variations in the ATS and EATS values (for standardized shifts ≤ 0.2) when the process standard deviation changes. The implementation of the VSI EWMA t - AI chart is illustrated using numerical examples. The third objective of this thesis is to investigate the economic and economic-statistical performances of the $\bar{X}$ - AI, synthetic $\bar{X}$ - AI and EWMA $\bar{X}$ - AI charts. The computation of optimal parameters of the aforementioned charts using the optimization algorithms and the details of the charts' economic and economic-statistical designs are also discussed in the thesis. The ARL and EARL criteria are used in setting the in-control and out-of-control statistical performances of these charts. By incorporating the economic and economic-statistical designs into the $\bar{X}$ - AI, synthetic $\bar{X}$ - AI and EWMA $\bar{X}$ - AI charts, the costs in implementing these charts can be minimized.

CHAPTER 1
INTRODUCTION

1.1 An Overview of Statistical Process Control (SPC)

To keep making progress in our daily lives, quality is what all of us want to get and to offer. The term *quality* is a multifaceted concept. Quality is dynamic as its definition varies according to the evolution of industries, as well as consumers' expectations over time. For instance, the quality of the image captured by a mobile phone a decade ago could not be better than the image captured by today's mobile phone. The traditional definition of quality is "fitness of use", while the modern definition is "Quality is inversely proportional to variability" (Montgomery, 2012). To reduce the cost due to scrap, rework and rejection in manufacturing, the concept of *quality* leads to *quality improvement*, which means "reduction of variability in processes and products" (Montgomery, 2012).

To ensure that good quality products are produced and services provided, one of the statistical methodologies in quality control, namely Statistical Process Control (SPC) was developed. SPC is a collection of statistical tools that are used to maintain quality; as well as to achieve quality improvement by reducing variability in the process. There are two causes of variation, i.e. the common (or natural) causes of variation and assignable (or special) causes of variation that occur in a process. The common causes of variation will always exist in the production process regardless of how good the design is. This type of variability is caused by the accumulation of many small and uncontrollable causes and it cannot be removed without changing the process. Thus, a process is said to be statistically in-control if only common causes of variation is present. On the other hand, the presence of assignable causes of variation is caused by operator errors, defective raw materials and machine errors. This type of variability is usually large and will lead to non-conforming items being produced. Therefore, a process is declared as out-of-control whenever an assignable cause is detected.

Seven statistical process monitoring tools are used in SPC. These tools are known as the magnificent seven, which include histogram, scatter plot, check sheet, Pareto chart, cause and effect diagram, defect concentration diagram and control chart (Montgomery, 2012). Histogram and scatter plot are graphical methods used to provide information on the distribution of the data and the relationship between two variables, respectively. A check sheet is used to gather historical or current operating data for the process under study in order to assist practitioners in diagnosing the cause of the defects. A Pareto chart is used to identify the most serious defect by showing the frequency of the defects in a systematic way. Subsequently, a cause and effect diagram is used to identify the potential causes that lead to the defects. To assist in identifying the potential causes of defects, the defect concentration diagram is used to show the different types of defects on the item.

Control chart is one of the most commonly used tools adopted in manufacturing and service industries as a monitoring tool to measure, monitor and improve process quality by identifying the occurrence of anomalies in the mean or variance of the process under study. The control charting concept was introduced by Walter. A. Shewhart of Bell Telephone Laboratories in 1924 (Montgomery, 2012). A control chart consists of the center line (CL), upper control limit (UCL) and lower control limit (LCL). The UCL and LCL are used to determine the state of the process being monitored, i.e. either in-control or out-of-control. If an unusual source of variation is present during process monitoring, the control charting statistics will be plotted beyond UCL and LCL, and the process is declared as out-of-control, otherwise, the process is in-control. The implementation of a control chart is important to practitioners in monitoring and improving the quality of the process and products effectively. In general, control charts are divided into two major types, i.e. variables control charts and attributes control charts. A variable control chart is used when the charted data are measurable, in terms of continuous values; whereas, an attribute control chart is adopted when the charted data are in the form of discrete counts, such as the number of conforming or non-conforming items (Gitlow et al., 1995).

In the 21st century, there has been a resurgent in the interest of investigating the performances of control charts that incorporated adaptive schemes and auxiliary information concept. Adaptive schemes refer to control charts where the sampling interval, sample size or both sampling interval and sample size are varied according to the performance of the current process. On the other hand, the auxiliary information concept is based on an estimator that contains information of more than one variable, i.e. the auxiliary and study variables to detect process shifts in the study variable more efficiently.

1.2 Problem Statement

Traditionally, the performance of a control chart is influenced by only the information from the quality characteristic of interest (study variable). Some control charts developed recently require information from an additional variable, called the auxiliary variable, that is correlated with the study variable in improving the performance of the aforementioned charts. In addition, a single sampling plan that relies only on the information from the study variable may not give a precisie estimator in estimating the population mean of the study variable if the sample size is not large enough due to cost constraint. In such circumstances, considering information from both the study and auxiliary variables will help in improving the precision of the mean estimator of the study variable (Haq and Khoo, 2018). Therefore, the need to develop new auxiliary information based control charts arises.

It is widely known that the Shewhart $\overline{X}$ chart's advantage lies in its simplicity and effectiveness in detecting large process mean shifts (Wu and Jiao, 2008; Saha 2018). However, in many applications, a quick detection of small and moderate shifts is important. Champ and Rigdon (1997) showed that the zone (or run sum) chart is as competitive as the cumulative sum (CUSUM) and exponentially weighted moving average (EWMA) charts by Page (1954) and Roberts (1959), respectively, in detecting small and moderate shifts. To the best of our knowledge, all existing literature on run sum charts only considered information from the study variable in process monitoring. Thus, to improve the process monitoring ability of run sum charts, it is vital to develop a new run sum $\overline{X}$ chart that incorporates an efficient estimator of the study variable, where information from both study and auxiliary variables are incorporated into the new chart's statistic.

It is known that the run length performance of the $\overline{X}$ type chart is significantly affected by changes in the process standard deviation, which will make the chart oversensitive or insensitive in detecting process shifts. To minimize the effect of changes (or estimation error) in the process standard deviation on the performance of $\overline{X}$ charts, Zhang et al. (2009) proposed the *t* and EWMA *t* charts for monitoring the process mean. More recently, Haq et al. (2019) proposed an auxiliary information based EWMA *t* chart for the process mean. Numerous research works have shown that incorporating the adaptive scheme into control charts will improve the performance of the basic charts in the detection of out-of-control signals (see Reynolds et al., 1988; Epprecht et al., 2010; Kazemzadeh et al., 2013 and Yeong et al., 2017). In order to enhance the performance of the EWMA t - AI chart, it is important to design an adaptive EWMA t - AI chart.

In real process monitoring scenarios, the process shift detection ability (or statistical performance) of a control chart is not only the sole concern of practitioners as the implementation cost of the chart is also taken into account by practitioners. The statistical performance of a control chart is evaluated in terms of the number of sample points (for a non-adaptive chart) or time (for an adaptive chart) required by the said chart to detect a process shift. This will not always yield the minimum cost in process monitoring (Surtihadi and Raghavachari, 1994). In view of this drawback, the economic design of a control chart which takes into account of the cost consideration, i.e. by minimizing the cost, in order to maximize profit was developed (Duncan, 1956; Lee and Khoo, 2018; Katebi and Moghadam, 2019). Nevertheless, the economic design ignores the statistical performance of the control chart which leads to more frequent false alarms or a higher Type-I error probability (Woodall, 1986). To reduce the Type 1-error probability, Saniga (1989) proposed the economic-statistical design of a control chart by integrating statistical properties into the economic design of the chart. Thus, it is crucial for practitioners to investigate the cost of implementation of a control chart in process monitoring. This can be attained by developing economic and economic-statistical designs in minimizing the cost of implementing control charts.

1.3 Scope and Limitations

The scope of this thesis lies in the development of new control charts with better performances than existing ones for the detection of out-of-control signals. Therefore, this thesis focuses in the development of various types of charts that integrate the auxiliary information concept with the control charting statistics. The limitations of the charts developed in this thesis are (i) only a single auxiliary variable is considered in the design of the charts, (ii) the bivariate normal distribution is assumed for all the auxiliary information based charts developed and (iii) simulated data are used to illustrate the applications of the proposed charts.

1.4 Objectives of the Thesis

The main objectives of this thesis are as follows:

(i) To develop the run sum $\overline{X}$ auxiliary information (RS $\overline{X}$ - AI) chart for monitoring the process mean.

(ii) To develop the variable sampling interval (VSI) EWMA t auxiliary information (VSI EWMA t - AI) chart for monitoring the process mean.

(iii) To develop the economic and economic-statistical designs of the $\overline{X}$, EWMA $\overline{X}$ and synthetic $\overline{X}$ charts with auxiliary information.

1.5 Organization of the Thesis

This thesis consists of 6 chapters. The first chapter provides an overview of SPC, where the concept of SPC, as well as the basic charts are briefly discussed. This is followed by a discussion on the research motivation that gives rise to the main objectives in the thesis. Following that, the objectives and organization of the thesis are provided.

Chapter 2 elaborates the literature on related control charts, such as the $\overline{X}$, EWMA $\overline{X}$, synthetic $\overline{X}$ and EWMA t charts with auxiliary information, RS $\overline{X}$ and VSI EWMA t charts, as well as the economic and economic-statistical designs of control charts. The operation of these charts and their corresponding run length properties are explained. Additionally, this chapter also discusses the relevant performance measures used in the thesis.

In Chapter 3, the proposed RS $\bar{X}$ - AI chart is discussed. Guidelines for the construction of the optimal RS $\bar{X}$ - AI chart, as well as the optimal algorithms in obtaining the optimal parameters of the RS $\bar{X}$ - AI chart are presented. Additionally, performance comparisons involving the RS $\bar{X}$ - AI and competing charts, such as the Shewhart $\bar{X}$ auxiliary information (denoted as $\bar{X}$ - AI), EWMA $\bar{X}$ auxiliary information (denoted as EWMA $\bar{X}$ - AI) and synthetic $\bar{X}$ auxiliary information (denoted as SYN $\bar{X}$ - AI) charts are discussed. To show the implementation of the RS $\bar{X}$ - AI chart, an illustrative example is provided.

Chapter 4 discusses the proposed VSI EWMA t - AI chart. The construction and performance evaluation of the VSI EWMA t - AI chart are discussed. A numerical example is given to demonstrate the implementation of the chart. To show the superiority of the VSI EWMA t - AI chart over existing EWMA t - AI chart when the process standard deviation is in-control, a comparative study in terms of the ATS, SDTS and EATS criteria is conducted, where the results are discussed in detail. In addition, the performance comparisons among the VSI EWMA t - AI and existing EWMA t - AI and EWMA $\bar{X}$ charts are conducted when changes in the process standard deviation occur.

Chapter 5 presents the economic and economic-statistical designs of the $\bar{X}$ - AI, SYN $\bar{X}$ - AI and EWMA $\bar{X}$ - AI charts. The optimal algorithms in obtaining the optimal parameters and minimum cost for implementing these charts are discussed. The cost performances of these charts are studied to show the effect of the AI feature on the economic and economic-statistical designs of the charts.

Chapter 6 provides a conclusion that summarizes the contributions and findings in this thesis. Additionally, some recommendations for future research works are given.

The references and appendices are presented at the end of the thesis. The optimization programs written in the MATLAB software for the RS $\bar{X}$ - AI chart and those of the economic and economic-statistical designs of the $\bar{X}$ - AI, SYN $\bar{X}$ - AI and EWMA $\bar{X}$ - AI charts are provided in Appendices A, B, C and D, respectively. The Monte Carlo simulation programs written in Statistical Analysis Software (SAS), for the VSI EWMA t - AI and RS $\bar{X}$ - AI charts are provided in Appendix E. Appendix F provides the MATLAB optimization and Monte Carlo simulation programs for the other charts under comparison.

CHAPTER 2
LITERATURE REVIEW

2.1 Introduction

This section begins with a review of existing control charts that are related to the proposed charts. The Shewhart $\bar{X}$ chart was proposed by Walter A. Shewhart at Bell Laboratories to help practitioners to attain quality improvements in the products produced and services offered by identifying special causes of variation in the process so that they are removed. The Shewhart $\bar{X}$ chart issues an out-of-control signal when a sample point falls beyond the control limits. The main setback of the Shewhart $\bar{X}$ chart is that it is slow in detecting small and moderate process mean shifts. To rectify this deficiency, auxiliary information control charts were proposed in the literature.

Section 2.2 presents a review of auxiliary information control charts. The auxiliary information concept is discussed in Section 2.2.1. The auxiliary information charts which are related to the aforementioned objectives 1 and 2 in Section 1.3 are discussed in Sections 2.2.2 – 2.2.5. These auxiliary information charts are the $\bar{X}$ - AI, EWMA $\bar{X}$ - AI, synthetic $\bar{X}$ - AI and EWMA t - AI charts. Additionally, the run sum $\bar{X}$ and VSI EWMA t charts which are also related to objectives 1 and 2 in Section 1.3 are discussed in Sections 2.3 and 2.4, respectively.

In Section 2.5, related economic and economic-statistical designs based control charts that are existing counterparts of objective 3 in Section 1.3 are discussed. The performance measures, such as average run length (ARL), expected average run length (EARL), average time to signal (ATS), standard deviation of the time to signal (SDTS) and expected average time to signal (EATS) used in evaluating the charts' performances are discussed in Section 2.6.

2.2 Auxiliary Information (AI) Charts

The auxiliary information approach involves the use of an efficient estimator that not only requires information from the study variable but also information from the correlated auxiliary variable(s) in improving the precision of the estimator (Riaz, 2008). The use of auxiliary information in designing a chart helps in enhancing the ability of the chart in detecting out-of-control signals as more information is integrated into the charting statistic. As an example, suppose that a pipe has both diameter (X) and length (Y) that together determine its breaking strength. If our interest is in monitoring the mean of the diameter, then the information from variables X and Y is used in the aforementioned efficient estimator in estimating the charting statistic. There are numerous studies in the literature that use the concept of auxiliary information in the design of control charts which consider the linear correlation between the study and auxiliary variables. The existing auxiliary information control charts will be discussed hereafter.

Riaz (2008) developed the Shewhart $\overline{X}$ chart for the mean using auxiliary information ($\overline{X}$ - AI), where the performance of the chart was shown to surpass the classical Shewhart $\overline{X}$ chart in detecting process mean shifts. By extending the work of Riaz (2008) that was based on the normality and known process parameters assumption, Riaz et al. (2013) investigated the effects of estimated process parameters on the $\overline{X}$ - AI chart under the normal and non-normal distributions. However, the control charts suggested by Riaz (2008) and Riaz et al. (2013) are less sensitive towards the detection of small and moderate shifts. Since the classical EWMA chart is known to provide superior performance in detecting small and moderate mean shifts, Abbas et al. (2014) proposed an auxiliary information based EWMA (EWMA $\overline{X}$ - AI) chart for monitoring the process mean. Abbas et al. (2014) showed that the EWMA $\bar{X}$ - AI chart outperforms the classical CUSUM and EWMA charts.

Haq and Khoo (2016) proposed the synthetic $\bar{X}$ (SYN $\bar{X}$) chart using auxiliary information (SYN $\bar{X}$ - AI) for monitoring the process mean. They showed that the SYN $\bar{X}$ - AI chart outperforms the basic SYN $\bar{X}$ chart in the detection of shifts for all values of correlation coefficient (ρ). The SYN $\bar{X}$ - AI chart also outperforms the EWMA $\bar{X}$ - AI chart for all shift sizes when $\rho \geq 0.9$. Additionally, Ahmad et al. (2014b) and Ahmad et al. (2014c) proposed the auxiliary information median and double sampling median charts, respectively.

More recently, Haq (2017) developed the synthetic EWMA and synthetic CUSUM charts by using regression-type estimator for the process mean, where the run length performances of the proposed charts were shown to surpass that of the classical synthetic EWMA, synthetic CUSUM, EWMA and CUSUM charts. Sanusi et al. (2017) presented an EWMA $\bar{X}$ chart by using ratio estimator, where the chart's performance was shown to be slightly inferior to the EWMA $\bar{X}$ - AI chart developed by Abbas et al. (2014) but performed better than the classical EWMA $\bar{X}$ and mixed EWMA - CUSUM charts especially when the study variable is strongly positively correlated with the auxiliary variable. In a similar vein, Sanusi et al. (2018) proposed the CUSUM-type location control chart by using the properties of auxiliary information in estimating the plotting statistics of the charts.

2.2.1 Auxiliary Information (AI) Technique

Assumed that a process consists of a quality characteristic of interest (study variable *X*) and an auxiliary characteristic *Y*. Let $\left(x_{r,1}, y_{r,1}\right), \left(x_{r,2}, y_{r,2}\right), \ldots, \left(x_{r,n}, y_{r,n}\right)$ be a bivariate random sample of size n, where r (= 1, 2, …) is the sample number. In addition, assume that each $(X_{r,j}, Y_{r,j})$ pair, for j =1,2,…,n, follows a bivariate normal distribution, i.e. $(X_{r,j}, Y_{r,j}) \sim N_2(\mu_X, \mu_Y, \sigma_X^2, \sigma_Y^2, \rho)$, where $\mu_X = \mu_{X0}$ when the underlying process of the study variable X is in-control, otherwise $\mu_X = \mu_{X1}$ when it is out-of-control; μ_Y is the population mean for the auxiliary variable Y, σ_X^2 and σ_Y^2 represent the population variance for the study variable X and auxiliary variable Y, respectively, and ρ is the correlation coefficient between variables X and Y. Let $\delta = \frac{|\mu_{X1} - \mu_{X0}|}{\sigma_X}$ is the magnitude of the standardized mean shift in the study variable X, where σ_X is the standard deviation of the study variable X, while μ_{X0} and μ_{X1} are the in-control and out-of-control process means of the study variable X, respectively. Following Riaz (2008), the regression estimator of μ_X is

$$\bar{X}_r^* = \bar{X}_r + \rho\left(\frac{\sigma_X}{\sigma_Y}\right)(\mu_Y - \bar{Y}_r), \tag{2.1}$$

where $\bar{X}_r = \sum_{j=1}^{n} X_{r,j}/n$ and $\bar{Y}_r = \sum_{j=1}^{n} Y_{r,j}/n$ are the r^{th} sample means of the study variable X and auxiliary variable Y, respectively.

The mean and variance of the regression estimator $\bar{X}_r^*$ are given as (Riaz, 2008)

$$E(\bar{X}_r^*) = \mu_X \tag{2.2}$$

and

$$\text{Var}(\bar{X}_r^*) = \frac{1}{n}\sigma_X^2(1 - \rho^2), \tag{2.3}$$

respectively. With the assumption of bivariate normality for the pair $(X_{r,j}, Y_{r,j})$, for r = 1, 2,… and j = 1, 2, …, n, $\bar{X}_r^*$ is a univariate normal random variable, i.e. $\bar{X}_r^* \sim N\left(\mu_X, \frac{1}{n}\sigma_X^2(1-\rho^2)\right)$ (Riaz, 2008).

2.2.2 Shewhart $\bar{X}$ Auxiliary Information ($\bar{X}$ - AI) Chart

The $\bar{X}$ - AI chart was proposed by Riaz (2008). It was shown to have a greater discriminatory power in detecting shifts than the basic $\bar{X}$ chart. The upper and lower control limits of the $\bar{X}$ - AI chart, i.e. $\text{UCL}_{(\bar{X}\text{ - AI})}$ and $\text{LCL}_{(\bar{X}\text{ - AI})}$, respectively, are computed as follows (Riaz, 2008):

$$\text{UCL}_{(\bar{X}\text{ - AI})} = \mu_{X0} + k_{(\bar{X}\text{ - AI})}\sigma_X\sqrt{\frac{1-\rho^2}{n_{(\bar{X}\text{ - AI})}}} \tag{2.4a}$$

and

$$\text{LCL}_{(\bar{X}\text{ - AI})} = \mu_{X0} - k_{(\bar{X}\text{ - AI})}\sigma_X\sqrt{\frac{1-\rho^2}{n_{(\bar{X}\text{ - AI})}}}, \tag{2.4b}$$

where $n_{(\bar{X}\text{ - AI})}$ and $k_{(\bar{X}\text{ - AI})}$ denote the sample size and control limit constant of the $\bar{X}$ - AI chart, respectively, while μ_{X0}, σ_X and ρ have been defined in Section 2.2.1. The $\bar{X}$ - AI chart signals an out-of-control at sample r when $\bar{X}_r^*$ in Equation (2.1) plots beyond the limits in Equations (2.4a) and (2.4b).

The ARL of the $\bar{X}$ - AI chart is obtained as (Haq et al., 2016)

$$\text{ARL}(\delta) = \frac{1}{P_{(\bar{X}\text{ - AI})}(\delta)}, \tag{2.5}$$

where

$$P_{(\bar{X}\text{ - AI})}(\delta) = 1 - \Phi\left(k_{(\bar{X}\text{ - AI})} - \delta\sqrt{n_{(\bar{X}\text{ - AI})}\big/(1-\rho^2)}\right) + \Phi\left(-k_{(\bar{X}\text{ - AI})} - \delta\sqrt{n_{(\bar{X}\text{ - AI})}\big/(1-\rho^2)}\right). \tag{2.6}$$

Here, δ is the shift size in the process mean and $\Phi(\cdot)$ is the cumulative distribution function (cdf) of the standard normal random variable. By letting $\delta = 0$ and $\delta > 0$ in Equation (2.5), the in-control and out-of-control ARLs, respectively, of the $\bar{X}$ - AI chart are obtained.

The EARL of the $\bar{X}$ - AI chart can be obtained as (Teoh et al., 2017)

$$\mathrm{EARL}\left(\delta_{\min}, \delta_{\max}\right) = \int_{\delta_{\min}}^{\delta_{\max}} f_{\delta}\left(\delta\right) \mathrm{ARL}\left(\delta\right)\, d\delta, \tag{2.7}$$

where $\delta_{\min}$ and $\delta_{\max}$ are the lower and upper bounds of the process mean shift interval, respectively, $f_{\delta}\left(\delta\right)$ is the probability density function (pdf) of δ, while $\mathrm{ARL}\left(\delta\right)$ for a specified value of δ is obtained using Equation (2.5). The distribution of δ is very difficult to approximate due to the sparse data for the out-of-control case. Furthermore, these data become obsolete when the assignable causes are detected and eliminated (Castagliola et al., 2011 and Teoh et al., 2017). Thus, δ is assumed to follow a uniform distribution on the interval $\left(\delta_{\min}, \delta_{\max}\right)$, where every value of δ in this interval has an equal probability of occurring. As a result, $\mathrm{EARL}\left(\delta_{\min}, \delta_{\max}\right)$ in Equation (2.7) becomes

$$\mathrm{EARL}\left(\delta_{\min}, \delta_{\max}\right) = \frac{1}{\delta_{\max} - \delta_{\min}} \int_{\delta_{\min}}^{\delta_{\max}} \mathrm{ARL}\left(\delta\right)\, d\delta. \tag{2.8}$$

Note that the in-control EARL is set to be equal to the in-control ARL. The MATLAB programs to compute the values of $\mathrm{ARL}\left(\delta\right)$ and $\mathrm{EARL}\left(\delta_{\min}, \delta_{\max}\right)$ of the $\bar{X}$ - AI chart are presented in Appendix F.1.

2.2.3 EWMA $\bar{X}$ Auxiliary Information (EWMA $\bar{X}$ - AI) Chart

Abbas et al. (2014) used the Monte Carlo simulation approach to evaluate their proposed EWMA $\bar{X}$ - AI chart, in terms of the ARL criterion. By using the estimator $\bar{X}_r^*$ in Equation (2.1), the charting statistic of the EWMA $\bar{X}$ - AI chart, for sample number $r = 1, 2, \ldots,$ is given as (Abbas et al., 2014)

$$Z_r = \lambda_{(\text{EWMA } \bar{X} \text{ - AI})} \bar{X}_r^* + \left(1 - \lambda_{(\text{EWMA } \bar{X} \text{ - AI})}\right) Z_{r-1}, \tag{2.9}$$

where $\lambda_{(\text{EWMA } \bar{X} \text{ - AI})} \in (0, 1]$ is the smoothing constant. Here, $\lambda_{(\text{EWMA } \bar{X} \text{ - AI})}$ is used to determine the depth of memory which is the degree of influence of older data (i.e. past sample means) towards the charting statistic. A smaller value of $\lambda_{(\text{EWMA } \bar{X} \text{ - AI})}$ indicates that past sample means have greater influence than the recent sample means; and a larger value of $\lambda_{(\text{EWMA } \bar{X} \text{ - AI})}$ indicates that recent sample means have greater influence than past sample means (Čisar and Čisar, 2011). According to Abbas et al. (2014), the initial value of the EWMA $\bar{X}$ - AI chart's statistic, Z_0, is set to be equal to the process target value, i.e. $Z_0 = \mu_{X0}$. It is also worth noting that the EWMA $\bar{X}$ - AI chart reduces to the $\bar{X}$ - AI chart when $\lambda_{(\text{EWMA } \bar{X} \text{ - AI})} = 1$.

The upper $\left(\text{UCL}_{(\text{EWMA } \bar{X} \text{ - AI})}\right)$ and lower $\left(\text{LCL}_{(\text{EWMA } \bar{X} \text{ - AI})}\right)$ control limits of the EWMA $\bar{X}$ - AI chart, based on the mean and variance of $\bar{X}_r^*$ in Equations (2.2) and (2.3), respectively, are shown as follows (Abbas et al., 2014):

$$\text{UCL}_{(\text{EWMA } \bar{X} \text{ - AI})} = \mu_{X0} + k_{(\text{EWMA } \bar{X} \text{ - AI})} \sigma_X \sqrt{\frac{\lambda_{(\text{EWMA } \bar{X} \text{ - AI})}\left(1 - \rho^2\right)}{n_{(\text{EWMA } \bar{X} \text{ - AI})}\left(2 - \lambda_{(\text{EWMA } \bar{X} \text{ - AI})}\right)}} \tag{2.10a}$$

and

$$\mathrm{LCL}_{(\mathrm{EWMA}\,\bar{X}\text{ - AI})} = \mu_{X0} - k_{(\mathrm{EWMA}\,\bar{X}\text{ - AI})}\sigma_X \sqrt{\frac{\lambda_{(\mathrm{EWMA}\,\bar{X}\text{ - AI})}\left(1-\rho^2\right)}{n_{(\mathrm{EWMA}\,\bar{X}\text{ - AI})}\left(2-\lambda_{(\mathrm{EWMA}\,\bar{X}\text{ - AI})}\right)}}, \qquad (2.10b)$$

where $n_{(\mathrm{EWMA}\,\bar{X}\text{ - AI})}$, $\lambda_{(\mathrm{EWMA}\,\bar{X}\text{ - AI})}$ and $k_{(\mathrm{EWMA}\,\bar{X}\text{ - AI})}$ represent the sample size, smoothing constant and limits' coefficient of the EWMA $\bar{X}$ - AI chart, respectively. Note that the ARL of the EWMA $\bar{X}$ - AI chart can be computed using the Markov chain model presented in Section 5.2.3, while the chart's EARL is obtained using Equation (2.8). The MATLAB optimization programs in minimizing the steady state $\mathrm{ARL}(\delta)$ and $\mathrm{EARL}(\delta_{\min}, \delta_{\max})$ values of the EWMA $\bar{X}$ - AI chart are provided in Appendix F.2.

2.2.4 Synthetic $\bar{X}$ Auxiliary Information (SYN $\bar{X}$ - AI) Chart

Wu and Spedding (2000) proposed the synthetic $\bar{X}$ (SYN $\bar{X}$) chart by integrating the Shewhart $\bar{X}$ and conforming run length ($\mathrm{CRL}_{(\mathrm{SYN}\,\bar{X})}$) sub-charts, which resulted in a significantly better detection power than the Shewhart $\bar{X}$ chart, for all shift sizes. Let $\mathrm{CRL}_{r\ (\mathrm{SYN}\,\bar{X})}$ represents the number of conforming samples between the $(r-1)^{\text{th}}$ and r^{th} nonconforming samples, inclusive of the ending r^{th} nonconforming sample, for the $\mathrm{CRL}_{(\mathrm{SYN}\,\bar{X})}$ sub-chart. Here, $\mathrm{CRL}_{r\ (\mathrm{SYN}\,\bar{X})}$ is used to decide whether a process is out-of-control. The process is out-of-control if $\mathrm{CRL}_{r\ (\mathrm{SYN}\,\bar{X})}$ is less than or equal to the lower limit of the $\mathrm{CRL}_{(\mathrm{SYN}\,\bar{X})}$ sub-chart, i.e. $\mathrm{CRL}_{r\ (\mathrm{SYN}\,\bar{X})} \leq L_{(\mathrm{SYN}\,\bar{X})}$, where $L_{(\mathrm{SYN}\,\bar{X})}$ is the lower limit of the $\mathrm{CRL}_{(\mathrm{SYN}\,\bar{X})}$ sub-chart. To further enhance the synthetic chart, Haq and Khoo (2016) integrated the AI concept into the SYN $\bar{X}$ chart, i.e. by integrating the $\bar{X}$ - AI and CRL sub-charts.

The $\text{UCL}_{(\bar{X}\text{ - AI})}$ and $\text{LCL}_{(\bar{X}\text{ - AI})}$ limits of the $\bar{X}$ - AI sub-chart are computed using Equations (2.4a) and (2.4b), respectively, but by replacing $k_{(\bar{X}\text{ - AI})}$ with $k_{(\text{SYN }\bar{X}\text{ - AI})}$, where $k_{(\text{SYN }\bar{X}\text{ - AI})}$ is the control limit constant of the SYN $\bar{X}$ - AI chart . The SYN $\bar{X}$ - AI chart is implemented by using the below step-by-step procedure.

Step 1: Compute the values of $\text{UCL}_{(\bar{X}\text{ - AI})}$ and $\text{LCL}_{(\bar{X}\text{ - AI})}$ of the $\bar{X}$ - AI sub-chart using Equations (2.4a) and (2.4b), respectively. Simultaneously, determine the value of the lower limit $L_{(\text{SYN }\bar{X}\text{ - AI})}$ for the CRL sub-chart ($\text{CRL}_{(\text{SYN }\bar{X}\text{ - AI})}$) of the SYN $\bar{X}$ - AI chart.

Step 2: Take a sample of size $n_{(\text{SYN }\bar{X}\text{ - AI})}$ and compute $\bar{X}_r^*$ using Equation (2.1). Note that $n_{(\text{SYN }\bar{X}\text{ - AI})}$ replaces n in Equation (2.1).

Step 3: If $\bar{X}_r^* \in \left[\text{LCL}_{(\bar{X}\text{ - AI})}, \text{UCL}_{(\bar{X}\text{ - AI})}\right]$, the sample is conforming. Then the control flow returns to Step 2. Otherwise, the control flow proceeds to Step 4.

Step 4: Determine the value of $\text{CRL}_{r\ (\text{SYN }\bar{X}\text{ - AI})}$, for $r = 1, 2, \ldots$, by counting the number of $\bar{X}_r^*$ samples between the $(r-1)^{\text{th}}$ and r^{th} nonconforming samples.

Step 5: If the value of $\text{CRL}_{r\ (\text{SYN }\bar{X}\text{ - AI})} > L_{(\text{SYN }\bar{X}\text{ - AI})}$, the process is in-control and the control flow returns to Step 2. Otherwise, an out-of-control signal is triggered and the control flow.

Figure 2.1 shows a summary of the above step-by-step procedure in the implementation of the SYN $\bar{X}$ - AI chart.

Both the zero state and steady state ARLs are used as performance mesures of the SYN $\bar{X}$ - AI chart. The zero state ARL is defined as the average number of sample points plotted on the chart from the start of process monitoring until the first out-of-

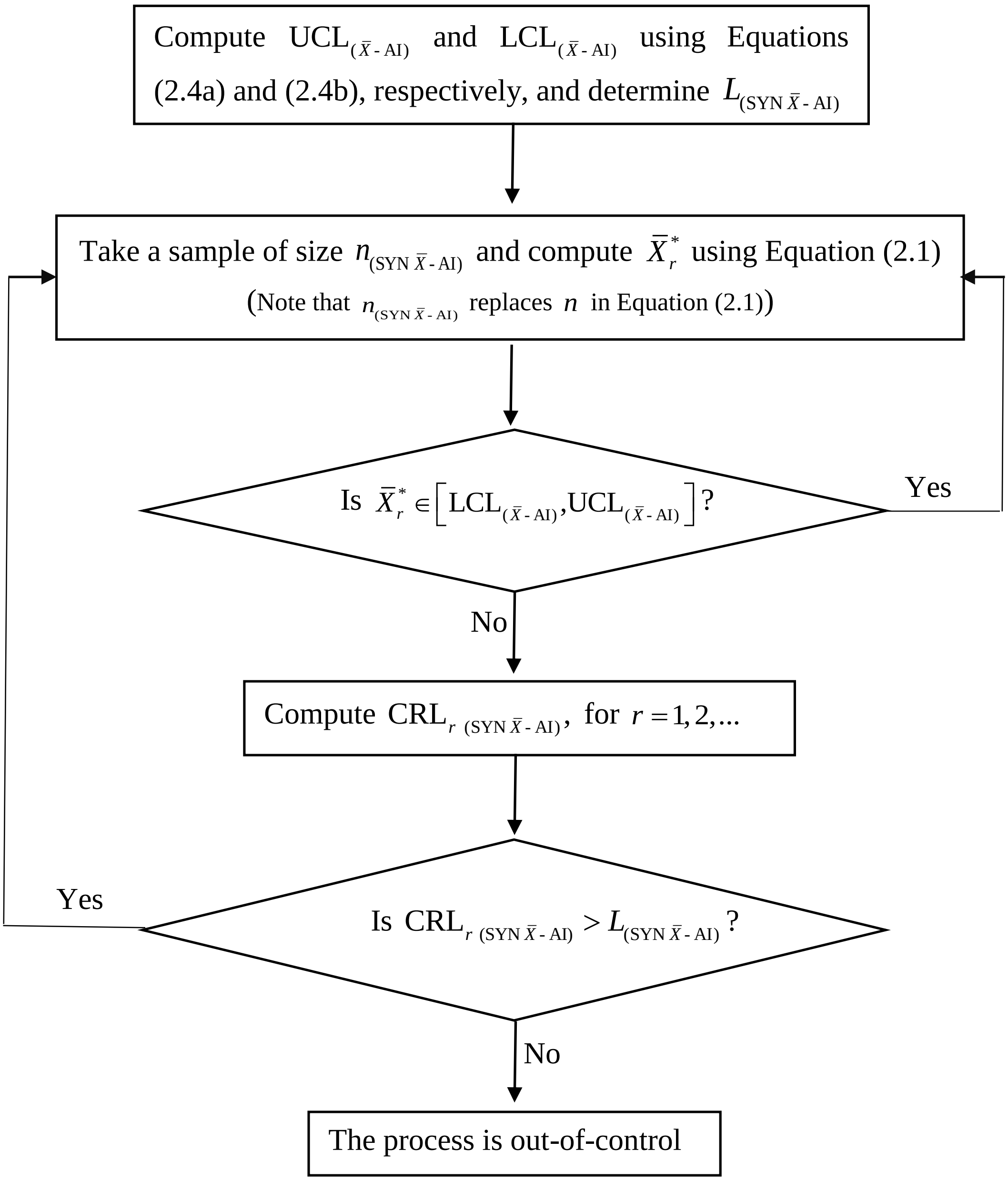

Figure 2.1 A procedure in the implementation of the SYN $\bar{X}$ - AI chart

control signal (due to the occurrence of a process shift) is detected. On the other hand, the steady state ARL is the average number of sample points plotted on the chart from the moment a process shift occurs at some random time after process monitoring begins until the first out-of-control signal (due to the occurrence of a process shift) is detected (Chew et al., 2015).

The zero state ARL of the SYN $\bar{X}$ - AI chart is obtained as (Haq and Khoo, 2016)

$$\mathrm{ARL}(\delta)=\frac{1}{P_{(\mathrm{SYN}\,\bar{X}\text{ - AI})}(\delta)}\times\frac{1}{\left(1-P_{(\mathrm{SYN}\,\bar{X}\text{ - AI})}(\delta)\right)^{L_{(\mathrm{SYN}\,\bar{X}\text{ - AI})}}}, \tag{2.11}$$

where

$$P_{(\mathrm{SYN}\,\bar{X}\text{ - AI})}(\delta)=1-\Phi\left(k_{(\mathrm{SYN}\,\bar{X}\text{ - AI})}-\delta\sqrt{n_{(\mathrm{SYN}\,\bar{X}\text{ - AI})}\Big/\left(1-\rho^2\right)}\right)+\Phi\left(-k_{(\mathrm{SYN}\,\bar{X}\text{ - AI})}-\delta\sqrt{n_{(\mathrm{SYN}\,\bar{X}\text{ - AI})}\Big/\left(1-\rho^2\right)}\right). \tag{2.12}$$

The steady state ARL of the SYN $\bar{X}$ - AI chart is computed using the Markov chain approach using Equation (2.13).

$$\mathrm{ARL}(\delta)=\boldsymbol{q}^T\left(\boldsymbol{I}-\boldsymbol{Q}_{(\mathrm{SYN}\,\bar{X}\text{ - AI})}\right)^{-1}\mathbf{1}. \tag{2.13}$$

Here, $\boldsymbol{q}$ is the steady state probability vector, $\boldsymbol{I}$ is an identity matrix, $\mathbf{1}$ is a column vector of all ones and $\boldsymbol{Q}_{(\mathrm{SYN}\,\bar{X}\text{ - AI})}$ is the transition probability matrix (tpm) for the transient states of the SYN $\bar{X}$ - AI chart. The vector $\boldsymbol{q}$ can be obtained by firstly solving $\boldsymbol{f}=\left(\boldsymbol{Q}^*_{(\mathrm{SYN}\,\bar{X}\text{ - AI})}\right)^T\boldsymbol{f}$ subject to $\mathbf{1}^T\boldsymbol{f}=1$, where $\boldsymbol{Q}^*_{(\mathrm{SYN}\,\bar{X}\text{ - AI})}$ is the tpm of the Markov chain model with the absorbing state. Then, compute the vector $\boldsymbol{f}^*$ by deleting the entry associated with the absorbing state in $\boldsymbol{f}$. Finally, $\boldsymbol{q}$ is computed as $\boldsymbol{q}=\left(\mathbf{1}^T\boldsymbol{f}^*\right)^{-1}\boldsymbol{f}^*$ (Saha et al., 2018). The tpm for the transient states, $\boldsymbol{Q}_{(\mathrm{SYN}\,\bar{X}\text{ - AI})}$, which is a square matrix with a dimension of $\left(L_{(\mathrm{SYN}\,\bar{X}\text{ - AI})}+1\right)\times\left(L_{(\mathrm{SYN}\,\bar{X}\text{ - AI})}+1\right)$ is obtained using the following step-by-step procedure (Haq and Khoo, 2016):

Step 1: The values in the first row of the first and second columns are computed as $1-P_{(\mathrm{SYN}\,\bar{X}\text{ - AI})}(\delta)$ and $P_{(\mathrm{SYN}\,\bar{X}\text{ - AI})}(\delta)$, respectively, where $P_{(\mathrm{SYN}\,\bar{X}\text{ - AI})}(\delta)$ is computed using Equation (2.12).

Step 2: The value in the last row of the first column is $1-P_{(\text{SYN}\,\bar{X}\text{ - AI})}(\delta)$.

Step 3: The diagonal entries for the other rows have the value $1-P_{(\text{SYN}\,\bar{X}\text{ - AI})}(\delta)$.

Step 4: The remaining entries have the value zero.

The in-control and out-of-control ARLs can be obtained by letting $\delta = 0$ and $\delta > 0$, respectively, in Equations (2.11) (for the zero state case) and (2.13) (for the steady state case). The zero state and steady state EARLs of the SYN $\bar{X}$ - AI chart are computed using Equation (2.8), except that $\text{ARL}(\delta)$ in Equation (2.7) is replaced by either the zero state $\text{ARL}(\delta)$ in Equation (2.11) or steady state $\text{ARL}(\delta)$ in Equation (2.13). Note that the definition of the steady state EARL is similar to that of the steady state ARL, except that the exact shift size, δ is replaced by the shift interval, $(\delta_{\min}, \delta_{\max})$ which encompasses the minimum and maximum shift sizes. The in-control zero state and steady state EARL values of the SYN $\bar{X}$ - AI chart are set to be equal to their respective in-control ARL values. The MATLAB optimization programs to minimize the steady state $\text{ARL}(\delta)$ and $\text{EARL}(\delta_{\min}, \delta_{\max})$ values of the SYN $\bar{X}$ - AI chart are shown in Appendix F.3.

2.2.5 EWMA *t* Auxiliary Information (EWMA *t* - AI) Chart

The auxiliary information based $\bar{X}$ - type charts are not robust against errors in estimating the process standard deviation, i.e. the $\bar{X}$ - type AI charts trigger an out-of-control situation whenever changes or estimation errors occur in the process standard deviation although the process mean is in-control. To overcome this problem, Haq et al. (2019) introduced the EWMA *t* - AI chart to monitor the process mean, where the chart's statistic does not require the estimation of the process standard deviation. The run length performance, in terms of the ARL, median run length (MRL) and standard deviation of the run length (SDRL), of the EWMA t - AI chart was shown to be substantially better than that of the EWMA t chart.

The plotting statistic of the EWMA t - AI chart, C_r, for sample $r = 1, 2, \ldots,$ is obtained as (Haq et al., 2019)

$$C_r = \lambda_{(\text{EWMA } t \text{ - AI})} t_r + \left(1 - \lambda_{(\text{EWMA } t \text{ - AI})}\right) C_{r-1}, \tag{2.14}$$

where $\lambda_{(\text{EWMA } t \text{ - AI})} \in (0,\ 1]$ is the smoothing constant and t_r is the Student's t statistic computed as

$$t_r = \frac{\sqrt{n_{(\text{EWMA } t \text{ -AI})}} \left(\bar{X}_r^* - \mu_{X0}\right)}{S_{X,r}\sqrt{1-\rho^2}}. \tag{2.15}$$

Here, t_r follows a Student's t - distribution with $n_{(\text{EWMA } t \text{ -AI})} - 1$ degrees of freedom if the underlying process is in-control, $S_{X,r} = \sqrt{\frac{1}{n_{(\text{EWMA } t \text{ - AI})} - 1} \sum_{j=1}^{n_{(\text{EWMA } t \text{ - AI})}} \left(X_{r,j} - \bar{X}_r\right)^2}$ is the sample standard deviation of the study variable X, for $r = 1, 2, \ldots,$ and $\bar{X}_r = \sum_{j=1}^{n_{(\text{EWMA } t \text{ - AI})}} X_{r,j} \big/ n_{(\text{EWMA } t \text{ - AI})}$, while $\bar{X}_r^*$, μ_{X0} and ρ have been defined in Section 2.2.1. The quantity C_{r-1} in Equation (2.14) represents the past information and the starting value of the charting statistic, C_0 is set to be equal to the process target value, i.e. $C_0 = \mu_{X0}$. Note that the EWMA t - AI chart reduces to the t - AI chart when $\lambda_{(\text{EWMA } t \text{ - AI})} = 1$.

The upper $\left(\text{UCL}_{(\text{EWMA } t \text{ - AI})}\right)$ and lower $\left(\text{LCL}_{(\text{EWMA } t \text{ - AI})}\right)$ control limits of the EWMA t - AI chart are (Haq et al., 2019)

$$\text{UCL}_{(\text{EWMA } t \text{ - AI})} = \mu_{X0} + k_{(\text{EWMA } t \text{ - AI})} \sqrt{\frac{\lambda_{(\text{EWMA } t \text{ - AI})}}{(2 - \lambda_{(\text{EWMA } t \text{ - AI})})} \cdot \frac{(n_{(\text{EWMA } t \text{ - AI})} - 1)}{(n_{(\text{EWMA } t \text{ - AI})} - 3)}} \tag{2.16a}$$

and

$$\text{LCL}_{(\text{EWMA } t \text{ - AI})} = \mu_{X0} - k_{(\text{EWMA } t \text{ - AI})}\sqrt{\frac{\lambda_{(\text{EWMA } t \text{ - AI})}}{\left(2-\lambda_{(\text{EWMA } t \text{ - AI})}\right)}\cdot\frac{\left(n_{(\text{EWMA } t \text{ - AI})}-1\right)}{\left(n_{(\text{EWMA } t \text{ - AI})}-3\right)}}, \tag{2.16b}$$

respectively, where $k_{(\text{EWMA } t \text{ - AI})}$ is the control limit constant of the EWMA *t* - AI chart and its value is selected to attain the desired in-control ARL, while $n_{(\text{EWMA } t\text{- AI})}$ is the sample size of the EWMA *t* - AI chart.

The operation of the EWMA *t* - AI chart is given as follows (Haq et al., 2019):

Step 1. Specify the values of the parameters μ_{X0}, μ_Y, σ_X^2, σ_Y^2, ρ, $n_{(\text{EWMA } t \text{ -AI})}$, $\lambda_{(\text{EWMA } t \text{ - AI})}$, δ and the in-control ARL value.

Step 2. Determine the value $k_{(\text{EWMA } t \text{ - AI})}$, based on the parameters specified in Step 1 using simulation. Also, compute $\text{UCL}_{(\text{EWMA } t \text{ - AI})}$ and $\text{LCL}_{(\text{EWMA } t \text{ - AI})}$ of the EWMA *t* - AI chart using Equations (2.16a) and (2.16b), respectively.

Step 3. If C_r in Equation (2.14) falls beyond the $\text{UCL}_{(\text{EWMA } t \text{ - AI})}$ and $\text{LCL}_{(\text{EWMA } t \text{ - AI})}$ limits, the process is declared as out-of-control. Otherwise, the process flow returns to Step 1.

Figure 2.2 shows a summary of the above step-by-step procedure in the implementation of the EWMA *t* - AI chart.

The SAS simulation programs to compute the ARL, SDRL and EARL values of the EWMA *t* - AI chart are provided in Appendix F.4.

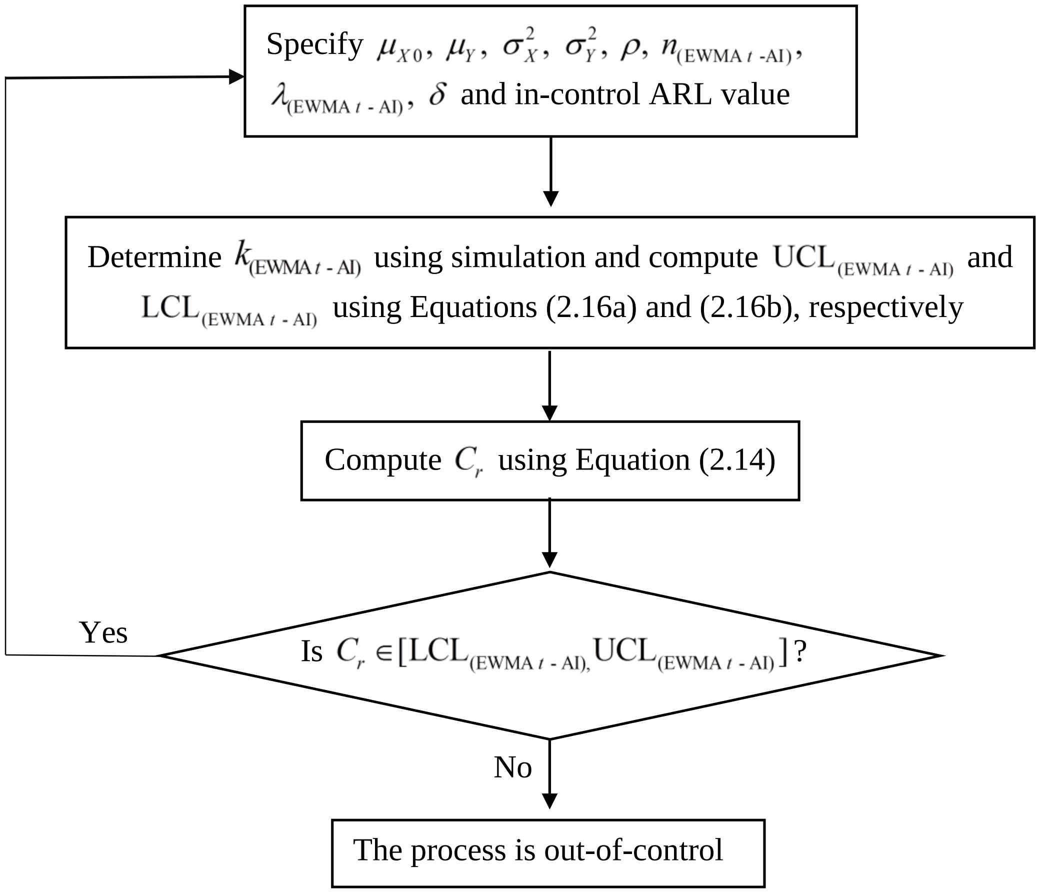

Figure 2.2 A procedure in the implementation of the EWMA *t* - AI chart

2.3 Run Sum (RS) $\bar{X}$ Chart

Jaehn (1987) introduced the zone chart for a quicker detection of an out-of-control situation, especially for the detection of small and moderate shifts in the process mean. The zone chart is also known as the run sum chart, where the chart is divided into several regions and each of the regions is assigned with an integer score. The RS $\bar{X}$ chart operates by giving an out-of-control signal when the cumulative score equals or exceeds a pre-defined triggering score. Davis et al. (1990) showed that the zone chart surpasses the Shewhart chart with common runs rules. To study the performance of a zone chart from an economic perspective, Ho and Case (1994) proposed an economic design of the zone chart for monitoring the process mean and variance, where the aforementioned chart was shown to outperform the economic design based $\bar{X}-R$ charts. Champ and Rigdon (1997) introduced the RS $\bar{X}$ chart, where the run length performance of the chart was studied using the Markov Chain approach. Champ and Rigdon (1997) pointed out that the performance of the RS $\bar{X}$ chart is as competitive as the EWMA and CUSUM charts if more regions are added to it. Figure 2.3 depicts a graphical view of the RS $\bar{X}$ chart.

As shown in Figure 2.3, the interval between the upper and lower control limits, i.e. $\mathrm{UCL}_{q\ (\mathrm{RS}\ \bar{X})}$ and $\mathrm{LCL}_{q\ (\mathrm{RS}\ \bar{X})}$, respectively, of the RS $\bar{X}$ chart is divided into $2q$ regions, having q regions above the center line $\left(\mathrm{CL}_{(\mathrm{RS}\ \bar{X})}\right)$, i.e. $R_{+1}, R_{+2}, ..., R_{+q}$, with the associated upper control limits $\mathrm{UCL}_{1\ (\mathrm{RS}\ \bar{X})} < \mathrm{UCL}_{2\ (\mathrm{RS}\ \bar{X})} < ... < \mathrm{UCL}_{q-1\ (\mathrm{RS}\ \bar{X})}$ $< \mathrm{UCL}_{q\ (\mathrm{RS}\ \bar{X})}\ (=\infty)$; and q regions below $\mathrm{CL}_{(\mathrm{RS}\ \bar{X})}$, i.e. $R_{-1}, R_{-2}, ..., R_{-q}$, with the associated lower control limits $\mathrm{LCL}_{q\ (\mathrm{RS}\ \bar{X})}\ (=-\infty) < \mathrm{LCL}_{q-1\ (\mathrm{RS}\ \bar{X})} < ... < \mathrm{LCL}_{2\ (\mathrm{RS}\ \bar{X})}$ $< \mathrm{LCL}_{1\ (\mathrm{RS}\ \bar{X})}$.

The positive integer scores and negative integer scores for the upper and lower regions are denoted as $\left(S_1, S_2, ..., S_q\right)$ and $\left(-S_1, -S_2, ..., -S_q\right)$, respectively. The upper and lower control limits, $\mathrm{UCL}_{k\ (\mathrm{RS}\ \bar{X})}$ and $\mathrm{LCL}_{k\ (\mathrm{RS}\ \bar{X})}$ of the RS $\bar{X}$ chart, for k = 1, 2, ..., $q-1$ are computed as (Chew et al., 2015)

$$\mathrm{UCL}_{k\ (\mathrm{RS}\ \bar{X})} = \mu_0 + M\left(\frac{3k}{q-1}\right)\frac{\sigma_0}{\sqrt{n_{(\mathrm{RS}\ \bar{X})}}} \tag{2.17a}$$

and

$$\mathrm{LCL}_{k\ (\mathrm{RS}\ \bar{X})} = \mu_0 - M\left(\frac{3k}{q-1}\right)\frac{\sigma_0}{\sqrt{n_{(\mathrm{RS}\ \bar{X})}}}, \tag{2.17b}$$